AGU PUBLICATIONS

*Journal of Advances in Modeling Earth System*

Supporting Information for

# Assessing Uncertainties and Approximations in Solar Heating of the Climate System

Juno C. Hsu, Michael J. Prather

Department of Earth System Science, University of California, Irvine CA USA

## Contents of this file



## Methods

Solar-J is based on Cloud-J (Prather, 2015) and has a long history of modeling and testing photolysis rates) for wavelengths 180-800 nm, which includes photolysis of $O_3$ and $NO_3$ in the 400-800 nm range (e.g., Olson et al, 1997; Photo Comp, 2010). For Solar-J, we adjusted the visible wavelength bands and adopted the RRTMG-SW spectral code for the infrared (see H2017). For wavelengths > 778 nm SJ simply takes the RR model. Since v7.5, SJ has shifted a wavelength boundary, 345-412-778 nm to 345-485-778 nm, to better separate the Rayleigh scattering region (345-485 nm) from the Chappuis ozone absorption (485-778 nm). We use the g-point sub-bins as specified for the 9 IR bands and as adapted to our last visible band (485-778 nm). In some test cases using alternative spectral models LLNL and CLIRAD, we have further reduced this latter band to 485-700 nm to match the IR bands of these two models.

The solar heating codes Solar-J and RRTMG-SW are included as modules within the UC Irvine chemistry-transport model (UCI CTM, Prather et al., 2017). The UCI CTM is coupled with meteorological fields from the European Centre Integrated Forecast System, open IFS cycle 38r1 run at T159N80L60 using the native Gaussian grid for atmospheric physics (about 1.1° horizontal with 60 layers). We take the archived 3-hour averages of the atmospheric column data: pressure on the layer edges; temperature, water vapor, cloud fraction, cloud liquid water content, cloud ice water content in each layer. A standard ozone climatology is used. Cloud effective radii (liquid and ice) and scattering phase function are as specified in the CTM photolysis code Cloud-J (Neu et al., 2007; Prather, 2015). The heating rates reported here are calculated for the IFS fields of January 2015. Cloud fields change every 3 hours, and the solar zenith changes every hour, giving 744 hourly data for January. The OSA code generously provided by Séférian was modified slightly: the diffuse albedo was not used as Solar-J calculates albedos specifically for each scattered stream; the albedo goes to a constant for SZA > 90° in spherical atmospheres; and the parameter table for the white-cap variable 'XRWC' was reset from 0.0 to 0.2 for wavelengths <400 nm.

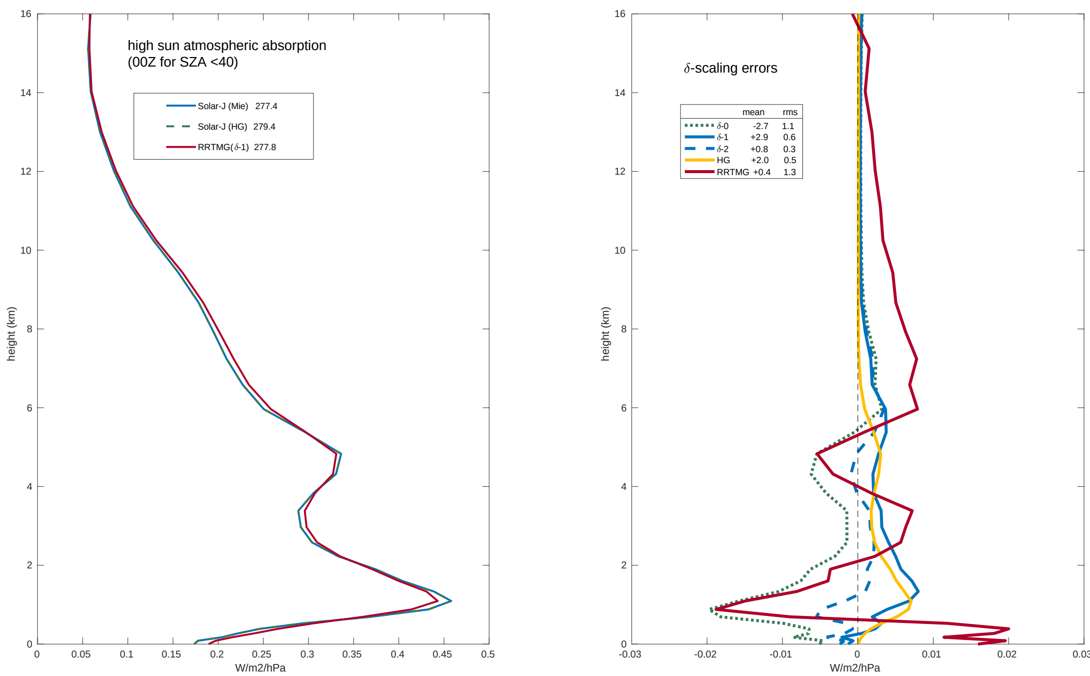


**Figure S1. (left)** January atmospheric absorption profiles (W $m^{-2}$ $hPa^{-1}$) over the Pacific Ocean at high sun (SZA > 40° at 00Z, area within green oval in Figure 4). Liquid-water, but not ice-water clouds are included. The total heating rates (W $m^{-2}$) for Solar-J with standard Mie phase function, Solar-J using a Henyey-Greenstein (HG) phase function, and RRTMG (standard δ-1 scaling) are shown in the legend. These values are averaged only over high sun. **(right)** Profiles of the errors in atmospheric absorption caused by δ-scaling (0, 1, 2) and HG phase function for liquid-water clouds. Same conditions as for left panel. Total heating-rate and rms differences (both W m-2) are given in the legend. Also shown is the difference, RRTMG (δ-1) minus Solar-J (Mie).

***(a)** SJ/2s–SJ(8s) clear sky*    ***(b)** SJ/2s/δ1–SJ/δ1 liq cld*    ***(c)** SJ/δ1ice–SJ all+QCA*

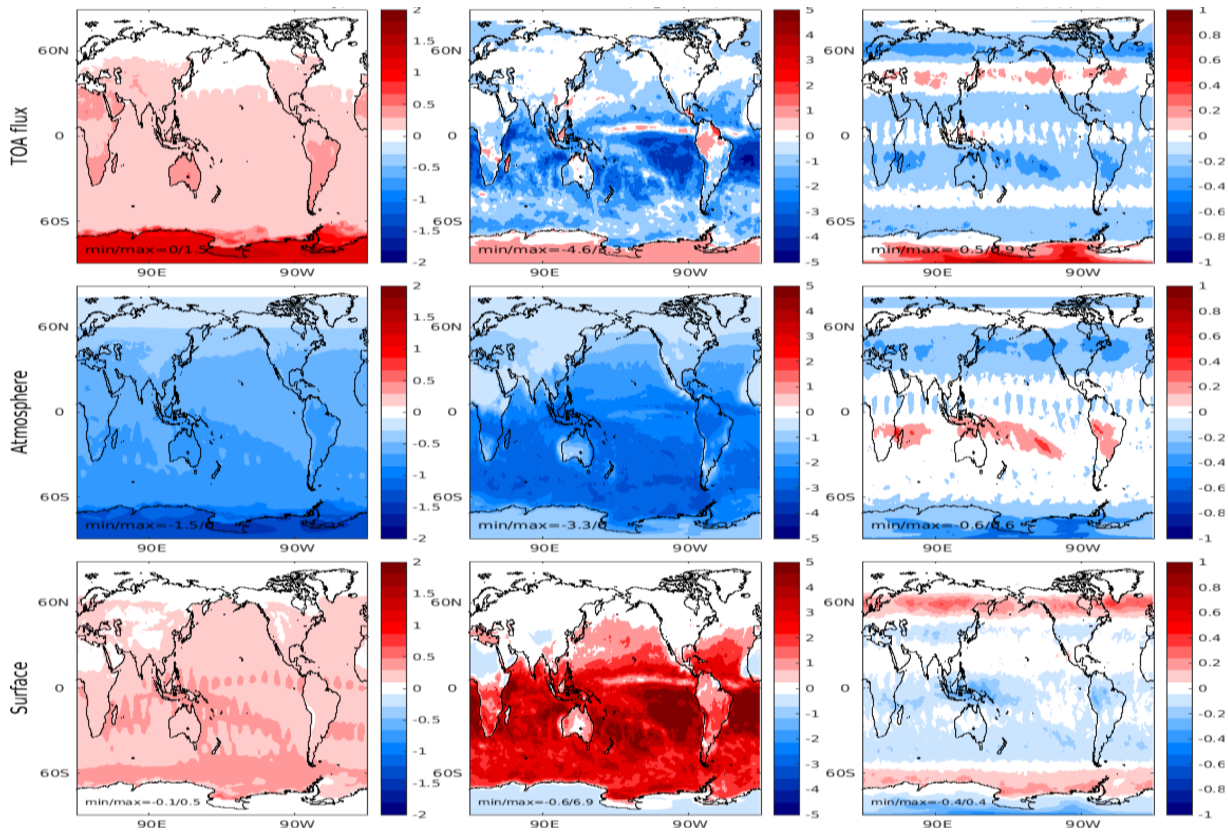


**Figure S2.** Geographic map of model differences in solar radiative budget (W $m^{-2}$) averaged over January, columns show **(a)** Solar-J's 2-stream minus 8-stream under clear sky, **(b)** Solar-J's 2-stream minus 8-stream with averaged liquid-only clouds and δ-1 scaling for both, and **(c)** Solar-J with δ-1 scaling of ice clouds minus the standard SJ where both calculations use ICAs sorted by cloud quadrature (QCA) and MAX-COR cloud overlap scheme. All calculations in this paper are aerosol-free. The small wave-24 noise seen in many of these panels results from calling the radiation code every hour.

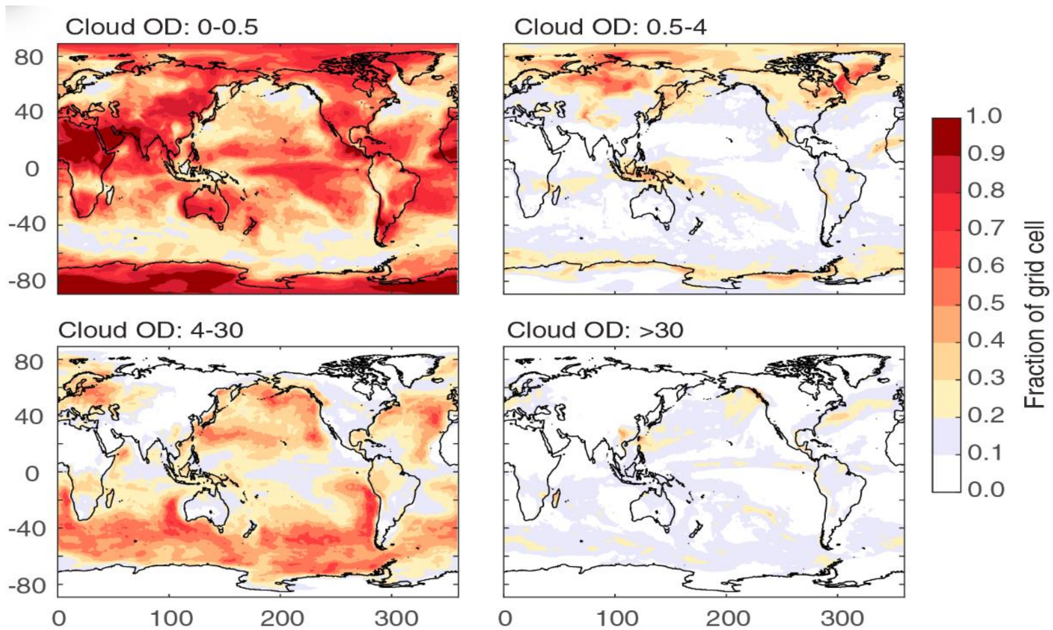


**Figure S3**. Frequency of occurrence for each of the four QCA bins using MAX-COR overlap for the January 2015 case study here. The QCAs are binned by 600 nm total cloud optical depth (liquid+ ice water: 0 – ½; ½ – 4; 4 – 30; >30. For each time step, the fractional area assigned to each QCA is calculated and then averaged over the month to give a frequency that sums to 1.00 over the 4 QCAs.

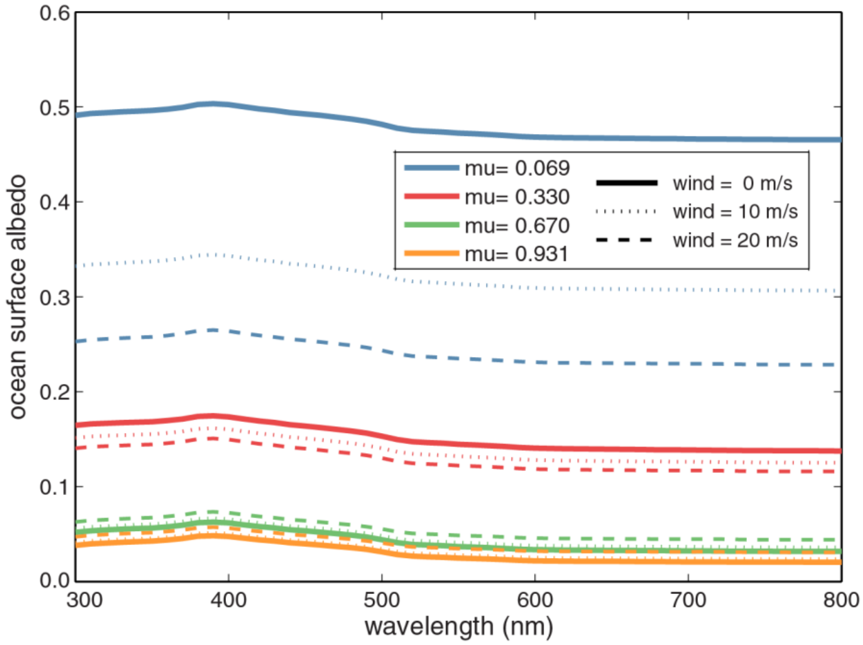


**Figure S4.** Ocean surface albedo (OSA, dimensionless) as a function of wavelength, shown for different incident angles (colors) and different wind speeds (solid, dashed or dotted). Four different incident zenith angles used in Solar-J's 8-stream scattering code are identified by their cosine values, mu: 0.931 (orange), 0.670 (green), 0.330 (red), 0.069 (blue). Three different wind speeds are shown: 0 m/s (solid), 10 m/s (dotted), 20 m/s (dashed).

**Table S1.** Versions of Solar-J and RRTMG-SW codes used here.

| notation | code description |
|---|---|
| SJ | The standard version of Solar-J version 7.6d as published here. It is a minor update of 7.6c published in Prather and Hsu (2019, doi.org/10.7280/D1096P) to make the MAX-RAN consistent with 7.6c changes. SJ uses a standard 8-stream Feautrier RT solver. Solar-J uses Cloud-J data tables for heating by $O_2$ (bins 1:11, <291 nm) & $O_3$ (bins 1:18, <778 nm) and RRTMG-SW tables for other gas-phase absorption ($H_2O$, $CO_2$, $CH_4$, $O_2$) in IR bands 18:27 (83 sub-bin g-points with 5 in visible and 78 in IR). Full cloud treatment includes vertical decorrelation length for cloud overlap (MAX-COR) to generate independent column atmospheres (ICAs) and then 4 cloud quadrature atmospheres (QCAs) to average over the ICAs. SJ can also be run with clear-sky or averaged cloud (full cloud cover in each cell as the average of cloudy and clear fractions), which does not invoke cloud-overlap and ICAs. SJ can be run in flat, spherical, refractive, and geometric options. SJ by default uses a constant ocean surface albedo (OSA = 0.06) but can invoke OSA to be of function of wavelength, incident angle (including scattered light) and surface wind. |
| SJ/RAN | SJ run with MAX-RAN cloud overlap. |
| SJ/RRX | The 78 IR sub-bins are replaced with the RRTM-SW benchmark code's 144 sub-bins. |
| SJ/CLIRAD | Solar-J with IR bands replaced with CLIRAD model: 0.70-1.22, 1.22-2.27, and 2.27-10.0 μm, each with 10 absorption sub-bins for each band (Chou and Suarez, 1996). The edge of the IR transition is shifted from 778 to 700 nm and cross section in bin 18 are adjusted. Only water vapor is included in the IR bands. |
| SJ/LLNL | The IR bands are replaced by the 3 large LLNL bands: 0.69–0.86, 0.86–2.27, and 2.27–3.85 μm, which include a total of 21 sub-bins. The edge of the IR transition is shifted from 778 to 700 nm and cross section in bin 18 are adjusted. Only water vapor is included in the IR bands. (Chou, 1992; Grant & Grossman, 1998). |
| SJ/hrv | SJ with high-resolution-visible version (*SJ/hrv*), putting 18 bands in the VIS region. |
| SJ/2S | SJ with 2-stream RT solver. |
| SJ/66b | SJ with a very high wavelength resolution in the IR used to resolve ice- and liquid-water cloud absorption. It is constructed using 0.05 to 0.10 μm wide bands, yielding 66 IR bands instead of the 9 in SJ. Without sub-bins, it cannot calculate any IR gas absorption. |
| SJ/Ray | SJ with the standard Rayleigh gas scattering phase function ($1 + \cos^2(\Theta)$) changed to isotropic (1). |
| SJ/δ0 | SJ with all cloud optical depths and phase functions changed to δ-0 scaling, see text and Table 2. |
| SJ/δ1 | SJ with all cloud optical depths and phase functions changed to δ-1 scaling, see text and Table 2. |
| SJ/δ1/2S | SJ/δ1 with 2-stream RT solver. |
| SJ/δ1ice | SJ standard, but with δ-1 scaling of ice clouds only. |
| SJ/δ2 | SJ with all cloud optical depths and phase functions changed to δ-2 scaling, see text and Table 2. |
| SJ/HG | SJ with all cloud phase functions changed to Henyey-Greenstein, see text and Table 2. |
| SJ/OSA | SJ with OSA a function of wavelength, incident angle (including scattered light) and surface wind. |
| AER4.0 | The standard RRTMG-SW version 4.0 code. If there are fractional clouds, this code uses MAX-RAN cloud overlap and McICA sampling of the ICAs. |

**Table S2.** Global monthly mean SW radiation budget for labeled experiments in Table 1. See Table S1 for the model version.

| name | Table 1 row | code version | conditions. | Incident | Reflected | Atmos. | Surface |
|---|---|---|---|---|---|---|---|
| B0 | 1-6, 17 | SJ (std) | flat-atmosphere, clear sky | 351.37 | 49.92 | 70.71 | 230.74 |
| B1 | 1 | SJ/CLIRAD | flat-atmosphere, clear sky | 351.37 | 50.86 | 65.03 | 235.47 |
| B2 | 2 | SJ/LLNL | flat-atmosphere, clear sky | 351.37 | 50.46 | 63.05 | 237.87 |
| B3 | 3 | SJ/RRX | flat-atmosphere, clear sky | 351.37 | 49.95 | 70.47 | 230.95 |
| B4 | 5 | SJ/hrv | flat-atmosphere, clear sky | 351.37 | 50.25 | 70.25 | 230.86 |
| B5 | 6 | SJ/2S | flat-atmosphere, clear sky | 351.37 | 50.23 | 70.18 | 230.96 |
| MR | 17 | SJ/Ray | flat-atmosphere, clear sky isotropic Rayleigh scattering | 351.37 | 49.91 | 70.72 | 230.74 |
| C0 | 7-8 | SJ/66b | sphere, QCA/MAX-COR overlap, no IR gases | 352.85 | 127.37 | 28.96 | 196.53 |
| C1 | 7 | SJ/CLIRAD | sphere, QCA/MAX-COR overlap, no IR gases | 352.86 | 125.23 | 32.80 | 194.83 |
| C2 | 8 | SJ | sphere, QCA/MAX-COR overlap, no IR gases | 352.89 | 126.23 | 30.64 | 196.02 |
| Mh | 9 | SJ/HG | flat-atmosphere, averaged clouds, no ice clouds | 351.45 | 127.26 | 78.31 | 145.88 |
| M0 | 9-14 | SJ | flat-atmosphere, averaged clouds, no ice clouds | 351.45 | 127.31 | 78.17 | 145.97 |
| M1 | 10 | SJ/δ0 | flat-atmosphere, averaged clouds, no ice clouds | 351.41 | 127.04 | 77.95 | 146.41 |
| M2 | 11,15 | SJ/δ1 | flat-atmosphere, averaged clouds, no ice clouds | 351.42 | 126.98 | 78.40 | 146.04 |
| M3 | 12 | SJ/δ2 | flat-atmosphere, averaged clouds, no ice clouds | 351.42 | 126.99 | 78.22 | 146.20 |
| M4 | 13,16 | SJ/δ1/2S | flat-atmosphere, averaged clouds, no ice clouds | 351.42 | 126.30 | 76.66 | 148.46 |
| M5 | 20 | SJ | flat-atmosphere, averaged clouds (all) | 351.46 | 131.19 | 78.49 | 141.77 |
| MI | 18 | SJ/δ1ice | flat-atmosphere, QCA/MAX-COR overlap | 351.43 | 111.57 | 76.88 | 162.98 |
| D0 | 18,19 | SJ | flat-atmosphere, QCA/MAX-COR cloud overlap | 351.43 | 111.59 | 76.87 | 162.97 |
| D1 | 19,21 | SJ/RAN | flat-atmosphere, QCA/MAX-RAN overlap | 351.43 | 110.24 | 76.81 | 164.38 |
| O0 | 22 | SJ/OSA | sphere, varied OSA | 352.98 | 111.72 | 76.77 | 164.49 |
| O1 | 22 | SJ | sphere, fixed OSA at 0.06 | 352.98 | 112.40 | 76.93 | 163.65 |
| | | | | | | | |
| RR0 | 4 | AER4.0 | clear sky | 351.38 | 51.22 | 70.24 | 229.92 |
| RR1 | 20 | AER4.0 | averaged clouds | 351.38 | 130.82 | 75.82 | 144.74 |
| RR2 | 14-16 | AER4.0 | averaged clouds, liquid only | 351.38 | 126.17 | 77.35 | 147.86 |
| RR3 | 21 | AER4.0 | McICA | 351.38 | 108.14 | 74.45 | 168.79 |

**Table S3**. Cross sections for ozone absorption and Rayleigh scattering in the 3 visible bands with different weighting functions

| | weighting | 320-345 nm | 345-485 nm | 485-778 nm |
|---|---|---|---|---|
| $\sigma_{Rayleigh}$ ($cm^2$) | Photons | 3.644e-26 | 1.387e-26 | 3.136e-27 |
| | Watts | 3.645e-26 (+0%) | 1.436e-26 (+4%) | 3.367e-27 (+7%) |
| $\tau_{Rayleigh}$ | | 0.73 | 0.29 | 0.07 |
| | | | | |
| $\sigma_{O3}$ ($cm^2$, 298 K) | Photons | 6.520e-21 | 2.125e-22 | 2.325e-21 |
| | Watts | 6.522e-21 (+0%) | 1.984e-22 | 2.427e-21 (+4%) |
| $\tau_{O3}$ (troposphere) | | 0.005 | 0.0002 | 0.002 |